Magnesium Technology 2011
Edited by: Wim H. Sillekens, Sean R. Agnew, Neale R. Neelameggham, and Suveen N. Mathaudhu
TMS (The Minerals, Metals & Materials Society), 2011

INHOMOGENEOUS DEFORMATION OF AZ31 MAGNESIUM SHEET IN UNIAXIAL TENSION

Jidong Kang[1], David S. Wilkinson[1], Raja K. Mishra[2]

[1]Department of Materials Science and Engineering, McMaster University,
1280 Main Street West, Hamilton, Ontario, L8S 4L7, Canada
[2]General Motors Research and Development Center,
30500 Mound Road, Warren, MI 48090-9055, USA

Keywords: magnesium alloy, plastic deformation, r-value, necking

Abstract

Inhomogeneous plastic deformation during uniaxial tensile test of AZ31 magnesium sheet has been studied using digital image correlation and electron backscatter diffraction techniques. It is shown that large strain gradients exist on the sheet surface parallel and perpendicular to the loading direction and very little deformation occurs in the thickness direction. The lack of thinning leads to abrupt fracture right after the formation of a premature but profound diffuse neck without transitioning to any localized neck. Such inhomogeneous deformation arises from the strong basal texture of the starting sheet and the resultant need for contraction and double twinning to accommodate strain. The strain distribution on the sheet surface evolves nonlinearly with strain, impacting the measured *r-value*.

Introduction

There is increasing interest in utilization of magnesium alloys in automotive applications due to their low density, superior specific tensile strength and rigidity compared to steel and aluminum alloys [1-2]. However, it is well recognized that the formability of wrought magnesium alloys at room temperature is inferior to that of steel and aluminum alloys. The poor formability of magnesium alloys is due to their hexagonal closed packed crystal structure and lack of many active slip systems at room temperature [1-2], requiring twinning to be activated.

The anisotropy of plasticity in Mg alloys affects yield asymmetry in tension and compression, the r-value (width to thickness strain ratio), and forming limit diagram, etc [3-8]. Most studies in the literature on the relationship between the mechanical properties and deformation mechanisms have relied on macroscopic stress-strain measurements and uniform strain assumptions in tensile gage length (common in studies of cubic metals such as steel and aluminum) to interpret microstructural observations in hexagonal Mg. For the first time, this study presents experimental data from simultaneous measurement of local strain and its evolution on the flat surface and the through thickness plane of the tensile sample using digital image correlation technique. Electron backscattered diffraction (EBSD) of the same surfaces is used to determine the nature of twinning accompanying the deformation. The dependence of the inhomogeneity of deformation on the deformation mechanism as well as the influence it has on the measurement of macroscopic r-values are discussed.

Experimental

A 2 mm thick AZ31 sheet material with nominal composition of 3 wt. % Aluminum and 1 wt. % Zinc was used in the present study. The sheets were annealed at 450 °C for 30 minutes in a vacuum furnace and air cooled to obtain a recrystallized starting microstructure. Uniaxial tensile tests were conducted at room temperate at a nominal strain rate of 6×10^{-4}/s. A commercially available optical strain measurement system, Aramis^{TD} [9], based on digital image correlation, was used to measure the surface strain during uniaxial tensile tests on both the sample surface and through-thickness plane simultaneously. The images were taken at a rate of 1 image per second.

A tapered sample was designed to investigate twinning during the tensile deformation. The test was stopped when maximum stress was reached in the tapered cross section. The sample was then cut into two halves at the center - the left part was mounted on the surface plane while the right part was mounted on the through thickness plane. The mounted samples were mechanically polished with 0.05 micron colloidal silica. The polished sample was first used for electron backscatter diffraction (EBSD) to determine the types of twins developed during the tensile tests and then etched using picric acid solution for optical microscopy to reveal twins in different regions.

For comparison, a strip cast 2mm thick AA5754 aluminum alloy sheet was tested for surface strain measurement on both surfaces in the present study.

Results and Discussion

The engineering stress – engineering strain curve for ASTM size sample of annealed AZ31 sheet pulled along the rolling direction (RD) is shown in Fig. 1. The data shows that there is an early onset of diffuse necking in this material followed by prolonged post necking deformation.

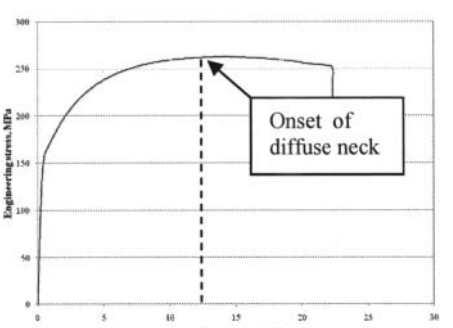

Fig. 1 Engineering stress – engineering strain curve of an AZ31 sheet material.

An examination of the DIC strain patterns on the surface during post diffuse necking stage of the deformation (Fig. 2 (a) (iv)-(vi)) shows that shear bands do not develop across the width of the sample. Fracture occurs right after a premature but profound diffuse necking without transitioning into localized necking.

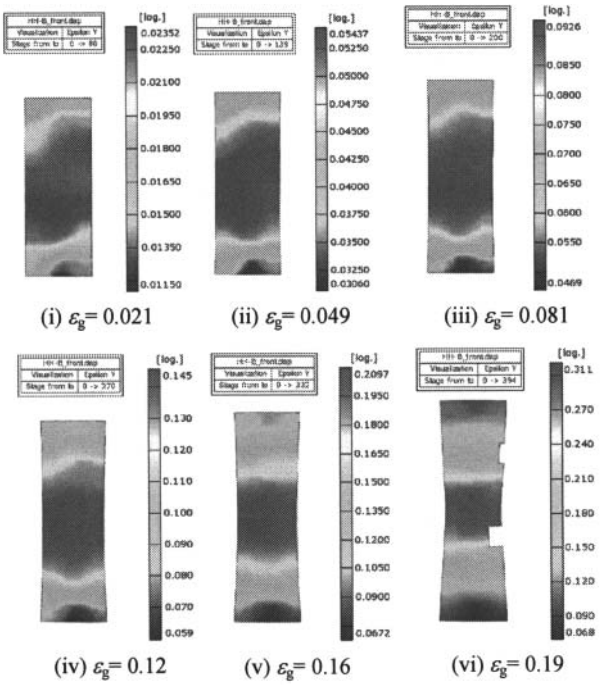

(a) Longitudinal strain

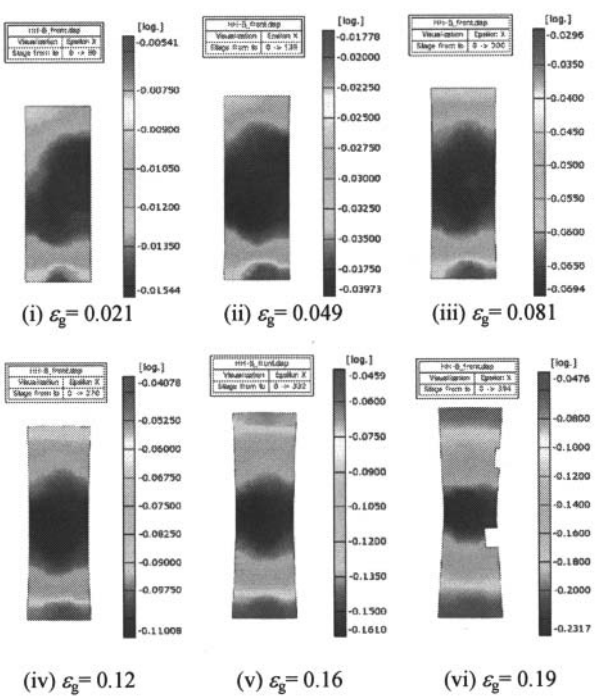

(b) width strain

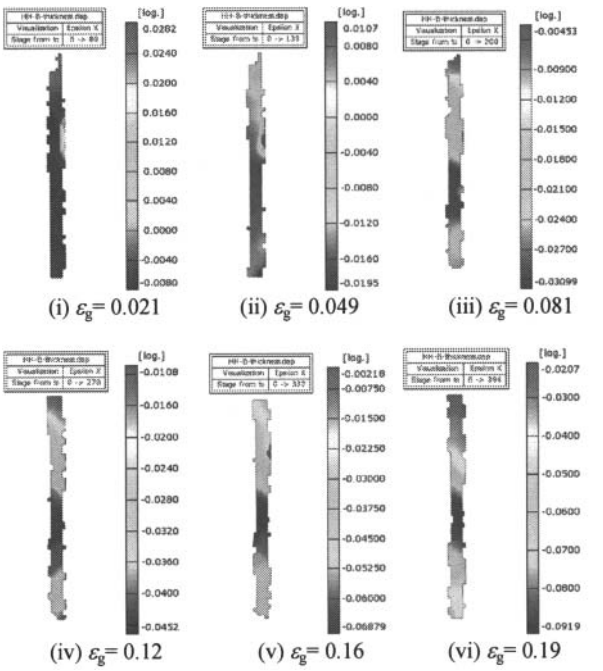

(c) thickness strain

Fig. 2 DIC maps showing the evolution of (a) longitudinal strain; (b) width strain and (c) thickness strain in a uniaxal tension sample of AZ31. ε_g represents global strain over a gage length of 25mm.

Data in Fig. 2 shows that both the longitudinal and width strains are non-uniformly distributed within the gage length. The nonlinearity of strain distribution is more evident in the line scan of longitudinal and width strains shown in Fig. 3. Both longitudinal and width strain at a given cross section keep evolving with global strain. The magnitude of the local width strain is nearly comparable to that of the longitudinal strain while the corresponding strain value in the thickness direction is very small. In other words, the necking process occurs in plane strain involving a narrowing process accompanied by minimal thinning.

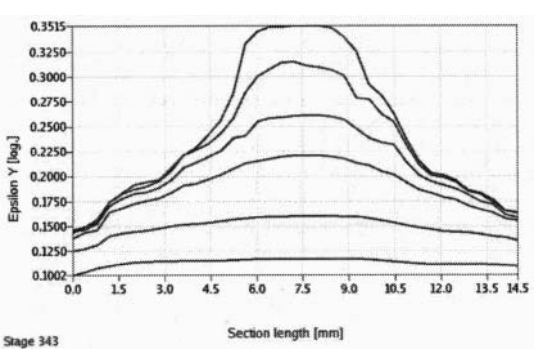

(a)

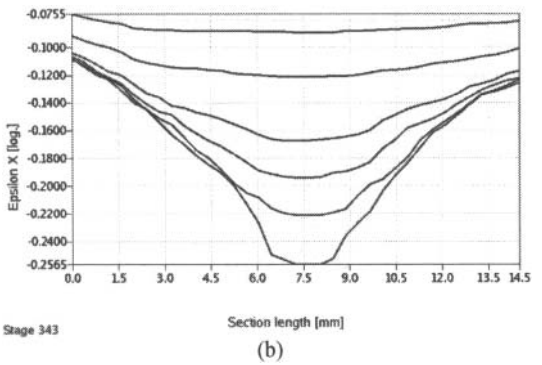

(b)

Fig. 3 Line scan of (a) longitudinal strain and (b) width strain at the center of the sample surface during "post diffuse neck" deformation in AZ31.

This data is to be contrasted with the evolution of local strain during uniaxial tensile testing of a strip cast AA5754 aluminum alloy sheet sample shown in Fig. 4. Strain within a narrow region increases with increasing global strain while strain outside this narrow region remains unchanged. The narrow region corresponds to the experimentally observed localized necking.

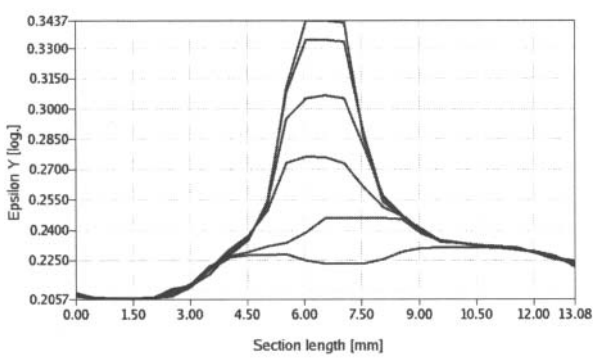

Fig. 4 Line scan of longitudinal strain during deformation in the "post diffuse neck" stage in AA5754 aluminum sheet. The strain gets localized when the shear band forms.

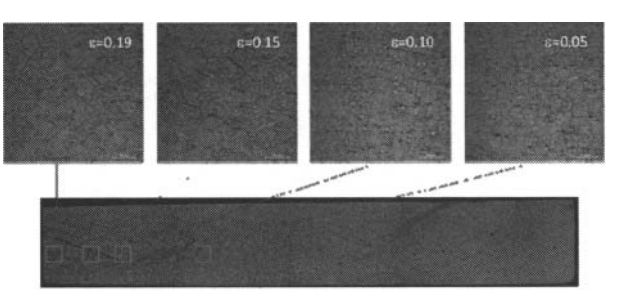

Fig. 5 Twinning development in a tapered AZ31 tensile sample.

Fig. 5 shows optical micrographs taken from the surface of a tapered sample deformed up to the necking strain in the tapered region. Images corresponding to regions with strains of 0.05, 0.10, 0.15 and 0.19 as measured by DIC show that even the region corresponding to a low strain value of 0.05 contains twins. The density of twins increases with increasing strain. Fig. 5 shows that twins tend to cluster by an auto catalytic process to form shear bands above a strain of 0.10. The shear bands get denser with increasing strain.

Electron back scatter diffraction (EBSD) data from these locations reveals that the location corresponding to the strain of 0.05 contains a number of grains deformed by extension twinning. Contraction twins are observed in areas corresponding to a strain of 0.10 or higher. The latter coincides with the onset of diffuse necking in the material. Contraction twins must form to accommodate the deformation in the thickness direction (which is along the c-axis). The low thickness strain measured by DIC is consistent with the observation of contraction twins which are difficult to form due to the high critical stress values needed for their formation, their low volume fraction and their clustering in closely spaced shear bands in the diffuse neck.

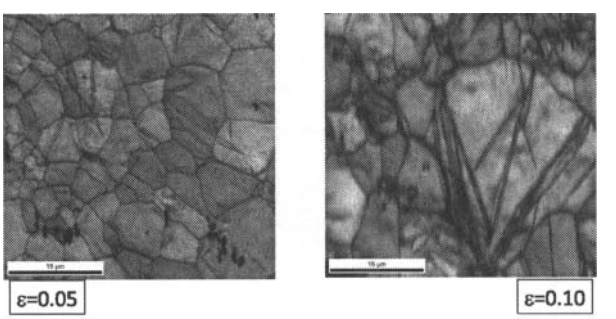

Fig. 6 Image quality maps from EBSD data showing extension twins with red boundaries. The dark straight lines are contraction and double twins (Jiang et al [10]).

The influence of the inhomogeneous deformation on mechanical properties of the material is revealed from the measurement of the anisotropy index, the so-called r-value, which is commonly defined as [11]

$$r = \frac{\varepsilon_w}{\varepsilon_t} = -\frac{\varepsilon_w}{\varepsilon_l + \varepsilon_w} \quad (1)$$

where $\varepsilon_l, \varepsilon_w, \varepsilon_t$ are longitudinal, width and thickness strains, respectively.

Thickness strain is difficult to measure using an extensometer during standard tensile testing. Two extensometers are usually used over a certain gage length in the longitudinal and width directions and incompressibility criterion along with the assumption of uniform strain distribution over the gage length is used to determine the r-value [11].

The current experimental method enables the independent measurement of all three strain components - the longitudinal, width and thickness strains at each point from which local r-value can be determined. Plots of the r-value evolution with global

strain based on strain measurements using i) longitudinal and width strains (commonly used); ii) longitudinal and thickness strains at different locations; and iii) longitudinal and width strains measured at a given point are shown in Fig. 7. "Gage length, Y, X" in Fig. 7 represents r-values calculated using strain measurements on the sample surface within the gage length in loading (Y) and width directions (X), thereafter referred to as Case 1; "Gage length, X, t(center)" and "Gage length, X, t(quarter)" represent r-values calculated using measured width strain and thickness strain in the center or quarter length in the sample, thereafter referred to as Case 2; "Point on surface, center, Y, X" and "Point on surface, quarter, Y, X" represent r-values calculated using strain measurements at selected points on sample surface in the center (within the necked area) or quarter length, thereafter referred to as Case 3.

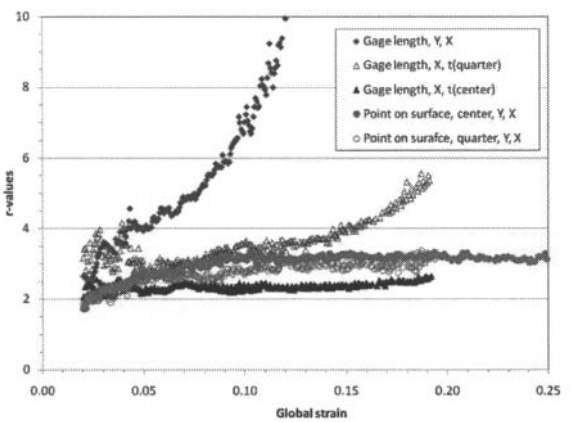

Fig. 7 Evolution of r-value with global strains in AZ31 based on different algorithms described in the text.

The r-values for Cases 1, 2 and 3 are quite different. In Case 1, r-value increases with increasing global strain, similar to what has been reported in the literature [7]. The variation of r-values with global strain for Case 2 is quite different. Since thickness strain is not uniformly distributed along the length direction of the sample, r-value varies with location of thickness strain. r-value data using strain values measured at "points" (Case 3) shows that r-value does not evolve above a strain of 0.10 regardless of the locations of the selected points, i.e. within or outside the necked area.

As shown in Fig. 2, the assumption of uniform strain in the gage section is not accurate, especially above 10% global strain. Since strain at a given point is calculated based on facet size in digital image correlation measurements, i.e. an actual spacing of 0.3mm in the present case, strain over this spacing can be regarded as macroscopically uniform. Therefore, r-value measurements based on "point" in Case 3, are consistent with the common definition of r-value. On the other hand, r-value data for Case 1 needs to be used with caution in view of the nonlinearity of strain distribution within the gage length in the longitudinal and width directions shown in Figs. 2 and 3.

The measured r-values using Case 1 and Case 3 criteria in AA5754 sheet material (Fig. 8) show no difference. Even with the existence of moving Portevin-Le Chatelier (PLC) bands in the Al-Mg alloy (AA5754 has 3 wt% Mg), the r-values based on strain measurements over the gage length tend to be constant beyond 10% strain, similar to the data in the literature [12-13].

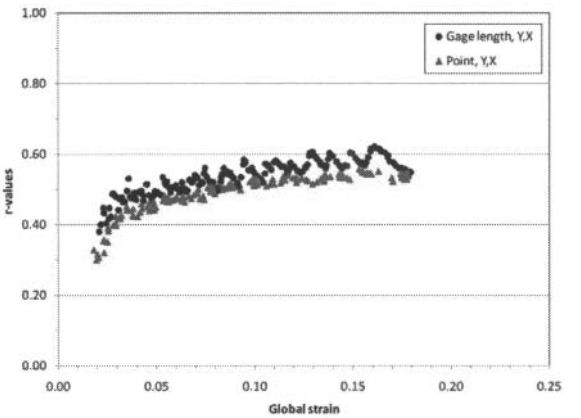

Fig. 8 Evolution of r-value with global strain in an AA5754 sheet material.

Summary

The inhomogeneous plastic deformation during uniaxial tensile test of an AZ31 magnesium sheet has been investigated using digital image correlation and electron backscatter diffraction.

(1) Very little deformation occurs in the thickness direction but large strain gradients exist on the sheet surface parallel and perpendicular to the loading direction during tensile deformation.
(2) The lack of thinning leads to the abrupt fracture right after a premature but profound diffuse necking without transitioning to localized necking.
(3) The observed inhomogeneous deformation arises from the strong basal texture and the necessity for the formation of contraction and double twins.
(4) *r-value* measurement in Mg alloys is shown to be sensitive to the method of measurement of the width and thickness strain. In view of the nonlinear evolution of strain distribution on the sheet surface, strain measured at "points" rather than "gage length" should be used to report r-values in Mg alloys.

Acknowledgements

The authors would like to acknowledge the support of the Resource for the Innovation of Engineering Materials program at the CANMET - Materials Technology Laboratory of Natural Resources Canada, and of Dr. Elhachmi Essadiqi in particular. Robert Kubic Jr. of GM R&D Center helped with EBSD measurements.

References

[1] Reed-Hill RE, Robertson WD. Acta Metall., 5 (1957) 728.
[2] Partridge PG. Metall Rev., 12(1967) 169.
[3] Wonsiewicz BC, Backofen WA. Trans of the Metall Society of AIME, 239 (1967) 1422.
[4] Kelly EW, Hosford WF. Trans of the Metall Society of AIME, 242 (1968) 5.

[5] Barnett MR, Keshavarz Z, Beer AG, Atwell D, Acta Mater. 52 (2004) 5093.
[6] Koike J. Metall and Mat Trans A, 36A (2005) 1689.
[7] Bohlen J, Nurnberg MR, Senn JW, Letzig D, Agnew SR. Acta Mater 55 (2007) 2101.
[8] Levesque J, Inal K, Neale KW, Mishra RK. Int J of Plasticity 26 (2010) 65.
[9] Aramis user manual, v.6, GOM mbH, Braunschweig, Germany, 2007.
[10] Jiang L. Scripta Mat, 54 (2006) 771.
[11] Hosford WF, Caddell RM, Metal Froming – Mechanics and Metallurgy (3rd edition), Cambridge University Press, 2007, p.207.
[12] Tong W. J Mech Phys Solids, 46 (1998) 2087.
[13] Kang J, Wilkinson DS, Embury JD, Jain M. SAE Transactions: J Mater and Manufacturing, 114 (2005) 156.